Panoptic Video Scene Graph Generation

Jingkang Yang[†], Wenxuan Peng[†], Xiangtai Li[†], Zujin Guo[†], Liangyu Chen[†], Bo Li[†]

Zheng Ma[‡], Kaiyang Zhou[†], Wayne Zhang[‡], Chen Change Loy[†], Ziwei Liu[†][✉]

[†]S-Lab, Nanyang Technological University, Singapore
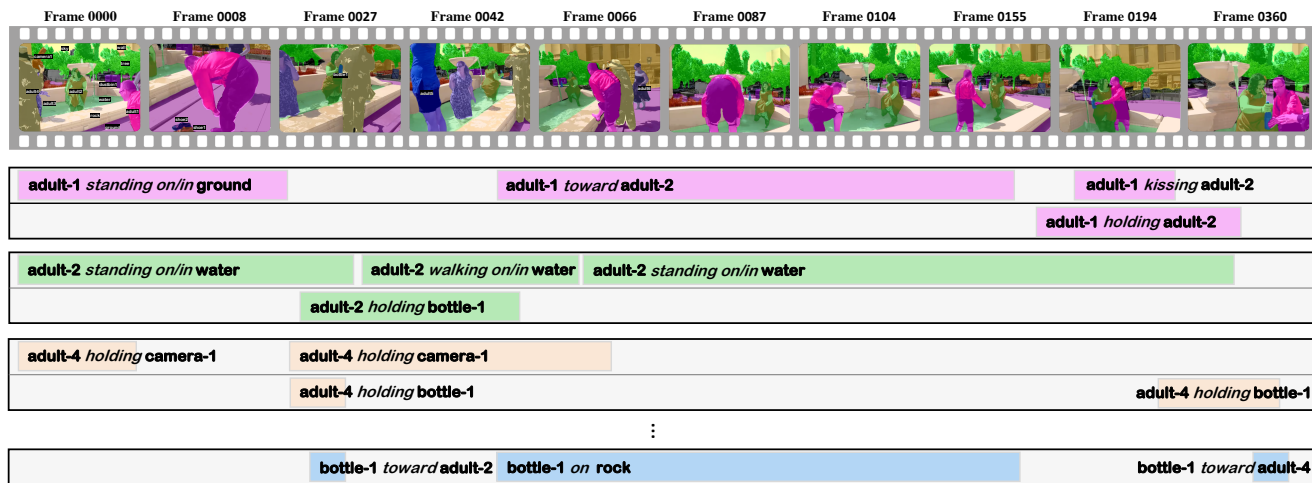[‡]SenseTime Research, Shenzhen, China

https:// n 0b w. o ibee oo .rest/Jingkang50/OpenPVSG

Figure 1. **An example video from our panoptic video scene graph (PVSG) dataset**. The top row shows some keyframes overlaid with the frame-wise panoptic segmentation masks. The timeline tubes underneath the keyframes contain fine, temporal scene graph annotations. The PVSG dataset contains 400 videos (with an average duration of 76.5 seconds), including 289 third-person and 111 egocentric videos.

Abstract

Towards building comprehensive real-world visual perception systems, we propose and study a new problem called panoptic scene graph generation (PVSG). PVSG is related to the existing video scene graph generation (VidSGG) problem, which focuses on temporal interactions between humans and objects localized with bounding boxes in videos. However, the limitation of bounding boxes in detecting non-rigid objects and backgrounds often causes VidSGG systems to miss key details that are crucial for comprehensive video understanding. In contrast, PVSG requires nodes in scene graphs to be grounded by more precise, pixel-level segmentation masks, which facilitate holistic scene understanding. To advance research in this new area, we contribute a high-quality PVSG dataset, which consists of 400 videos (289 third-person + 111 egocentric videos) with totally 150K frames labeled with panoptic segmentation masks as well as fine, temporal scene graphs. We
also provide a variety of baseline methods and share useful design practices for future work.

1. Introduction

In the last several years, scene graph generation has received increasing attention from the computer vision community [15, 16, 24, 48–51]. Compared with object-centric labels like "person" or "bike," or precise bounding boxes commonly seen in object detection, scene graphs provide far richer information in images, such as "a person riding a bike," which capture both objects and the pairwise relationships and/or interactions. A recent trend in the scene graph community is the shift from static, image-based scene graphs to temporal, video-level scene graphs [1, 41, 49]. This has marked an important step towards building more comprehensive visual perception systems.

Compared with individual images, videos clearly contain more information due to the additional temporal dimension,

Table 1. **Comparison between the PVSG dataset and some related datasets**. Specifically, we choose three video scene graph generation (VidSGG) datasets, three video panoptic segmentation (VPS) datasets, and two egocentric video datasets—one for short-term action anticipation (STA) while the other for video object segmentation (VOS). Our PVSG dataset is the first long-video dataset with rich annotations of panoptic segmentation masks and temporal scene graphs.

Dataset	Task	#Video	Video Hours	Avg. Len.	View	#ObjCls	#RelCls	Annotation	# Seg Frame	Year	Source
ImageNet-VidVRD [35]	VidSGG	1,000	-	-	3rd	35	132	Bounding Box	-	2017	ILVSRC2016-VID [33]
Action Genome [15]	VidSGG	10,000	99	35s	3rd	80	50	Bounding Box	-	2019	YFCC100M [42]
VidOR [34]	VidSGG	10,000	82	30s	3rd	35	25	Bounding Box	-	2020	Charades [36]
Cityscapes-VPS [17]	VPS	500	-	-	vehicle	19	-	Panoptic Seg.	3K	2020	-
KITTI-STEP [45]	VPS	50	-	-	vehicle	19	-	Panoptic Seg.	18K	2021	-
VIP-Seg [28]	VPS	3,536	5	5s	3rd	124	-	Panoptic Seg.	85K	2022	-
Ego4D-STA [12]	STA	1,498	111	264s	ego	-	-	Bounding Box	-	2022	-
VISOR [8]	VOS	179	36	720s	ego	257	2	Semantic Seg.	51K	2022	EPIC-KITCHENS [7]
PVSG	PVSG	400	9	77s	3rd + ego	126	57	Panoptic Seg.	150K	2023	VidOR + Ego4D + EPIC-KITCHENS

which largely facilitates high-level understanding of temporal events (e.g., actions [14]) and is useful for reasoning [59] and identifying causality [10] as well. However, we argue that current video scene graph representations based on bounding boxes still fall short of human visual perception due to the lack of *granularity*—which can be addressed with *panoptic segmentation masks*. This is echoed by the evolutionary path in visual perception research: from image-level labels (i.e., classification) to spatial locations (i.e., object detection) to more fine-grained, pixel-wise masks (i.e., panoptic segmentation [20]).

In this paper, we take scene graphs to the next level by proposing *panoptic video scene graph generation (PVSG)*, a new problem that requires each node in video scene graphs to be grounded by a pixel-level segmentation mask. Panoptic video scene graphs can solve a critical issue exposed in bounding box-based video scene graphs: both things and stuff classes (i.e., amorphous regions containing water, grass, etc.) can be well covered—the latter are crucial for understanding contexts but cannot be localized with bounding boxes. For instance, if we switch from panoptic video scene graphs to bounding box-based scene graphs for the video in Figure 1, some nontrivial relations useful for context understanding like "adult-1 standing on/in ground" and "adult-2 standing on/in water" will be missing. It is also worth noting that bounding box-based video scene graph annotations, at least in current research [15], often miss small but important details, such as the "candles" on cakes.

To help the community progress in this new area, we contribute a high-quality PVSG dataset, which consists of 400 videos among which 289 are third-person videos and 111 are egocentric videos. Each video contains an average length of 76.5 seconds. In total, 152,958 frames are labeled with fine panoptic segmentation and temporal scene graphs. There are 126 object classes and 57 relation classes. A more detailed comparison between our PVSG dataset and some related datasets is shown in Table 1.

To solve the PVSG problem, we propose a two-stage framework: the first stage produces a set of features for each

mask-based instance tracklet while the second stage generates video-level scene graphs based on tracklets' features. We study two design choices for the first stage: 1) a panoptic segmentation model + a tracking module; 2) an end-to-end video panoptic segmentation model. For the second scene graph generation stage, we provide four different implementations covering both convolution and Transformer-based methods.

In summary, we make the following contributions to the scene graph community:

1. **A new problem**: We identify several issues associated with current research in scene graph generation and propose a new problem, which combines video scene graph generation with panoptic segmentation for holistic video understanding.

2. **A new dataset**: A high-quality dataset with fine, temporal scene graph annotations and panoptic segmentation masks is proposed to advance the area of PVSG.

3. **New methods and a benchmark**: We propose a two-stage framework to address the PVSG problem and benchmark a variety of design ideas, from which valuable insights on good design practices are drawn for future work.

2. Related Work

Scene Graph Generation   Given an image, the scene graph generation (SGG) task expects the model to output a scene graph representation, where nodes represent objects and edges represent relations between objects. To localize object instances, the nodes should be grounded by the bounding boxes [48]. Classic scene graph generation methods have been dominated by the two-stage pipeline that consists of object detection and pairwise predicate estimation [38, 39, 48, 56, 58]. Recent works on one-stage methods [4, 23, 50] provide simpler models that output semantically diverse relation predictions. Though the prevalent
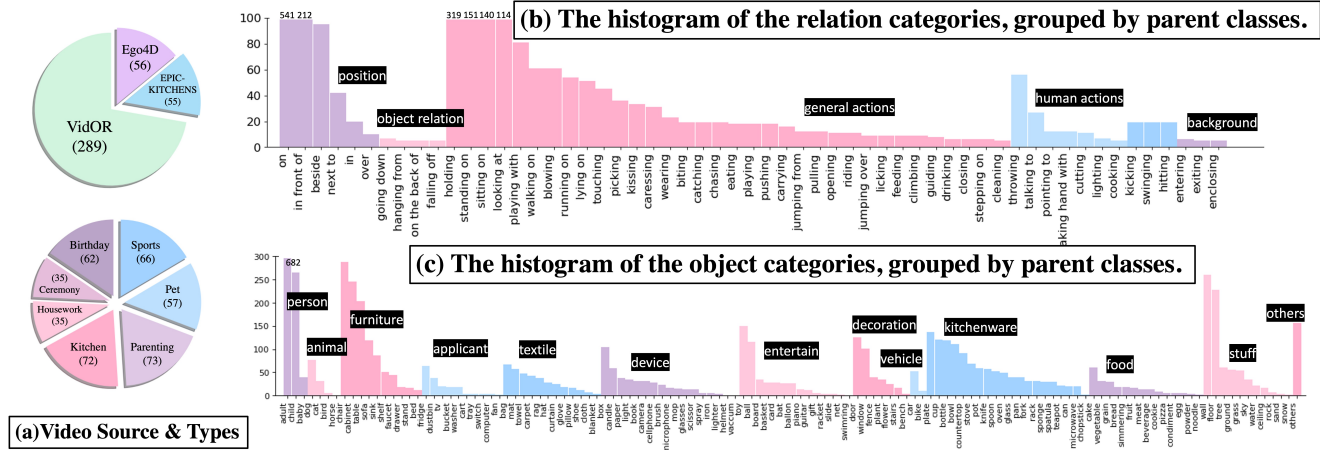
Figure 2. **The PVSG dataset statistics.** The PVSG dataset contains 400 third-person and ego-centric videos from diverse environments, as shown in (a). The statistics of object classes and relation classes are shown in (b) and (c).

SGG benchmark Visual Genome [21] provides rich annotations, it suffers from numerous "noisy" ground-truth predicate labels, e.g., some un-annotated negative samples are not absolutely background. NICE [22] reformulates SGG as a noisy label learning problem. They re-assign pseudo labels to detected noisy negative samples. Instead of exploiting the noisy SGG datasets, recently a new task of panoptic scene graph generation (PSG) [50] has been proposed with a refined PSG dataset, based on panoptic segmentation annotations to identify foreground and background concretely. Our work extends PSG to video level by predicting spatial-temporal relations.

Video Scene Graph Generation Shang *et al*. [35] first proposes Video Scene Graph Generation (VidSGG) and released ImageNet-VidVRD dataset. They generate object tracklet proposals and short term relations on overlapping segments. Subsequently, they greedily associate these relation triplets into video level. Several works follow the track-to-detect paradigm with spatio-temporal graph and graph convolutional neural networks [26, 31], or multiple hypothesis association [37]. MVSGG [49] investigates the spatio-temporal conditional bias problem in VidSGG. They perform a meta training and testing process, constructing the data distribution of each query set w.r.t. the conditional biases. TRACE [41] decouples the context modeling for relation prediction from the complicated low-level entity tracking. [1] raises the issue of domain shift between image and video scene graphs. They exploit external commonsense knowledge to infer the unseen dynamic relationship, and employ hierarchical adversarial learning to adapt from image to video data distributions. Embodied Semantic SGG [24] exploits the embodiment of the intelligent agent to autonomously generate an appropriate path by reinforcement learning [9] to explore an environment.

Video Panoptic Segmentation Video Panoptic Segmentation (VPS) [18, 28, 46] unifies both Video Semantic Segmentation [5] and Video Instance Segmentation [52] in one framework. It extends panoptic segmentation into video via making instance IDs across frames consistent. VPSNet [18] first extends cityscapes sequences [5] and builds a VPS dataset for driving scene, along with a new metric named Video Panoptic Quality (VPQ). STEP dataset [46] proposes another metric named Segmentation and Tracking Quality (STQ) that decouples the segmentation and tracking error. VIP-Seg [28] proposes a large scale VPS dataset which contains various scenes. Several works [18, 47, 55] are proposed to solve VPS task respectively. VIP-Deeplab [32] extends the Panoptic-Deeplab [2] with next frame center map prediction. Video K-Net [25] unifies the VPS pipeline via kernel online tracking and linking. TubeFormer [19] process tube-frames with temporal attention. Compared with previous VPS datasets, our PVSG dataset contains the extremely long videos, which bring new challenges for VPS tasks. Moreover, our work is beyond VPS tasks by also considering relation across a video.

3. The PVSG Problem

The goal of the PVSG problem is to describe a given video with a dynamic scene graph, with each node associated with an object and each edge associated with a relation in the temporal space. Formally, the input of the PVSG model is a video clip $\mathbf{V} \in \mathbb{R}^{T \times H \times W \times 3}$, where T denotes the number of frames, and the frame size $H \times W$ should be consistent across the video. The output is a dynamic scene graph $\mathbf{G}$. The PVSG task can be formulated as follows,

$$\Pr\left(\mathbf{G} \mid \mathbf{V}\right) = \Pr\left(\mathbf{M}, \mathbf{O}, \mathbf{R} \mid \mathbf{V}\right). \tag{1}$$

More specifically, $\mathbf{G}$ comprises the binary mask tubes $\mathbf{M} = \{\mathbf{m}_1, \ldots, \mathbf{m}_n\}$ and object labels $\mathbf{O} = \{o_1, \ldots, o_n\}$ that correspond to each of the n objects in the video, and their relations in the set $\mathbf{R} = \{r_1, \ldots, r_l\}$. For object i, the mask tube $\mathbf{m}_i \in \{0, 1\}^{T \times H \times W}$ collects all its tracked masks in each frame, and its object category should be $o_i \in \mathbb{C}^O$. For all objects in a frame t, the masks do not overlap, i.e., $\sum_{i=1}^{n} \mathbf{m}_i^t \leq \mathbf{1}^{H \times W}$. The relation $r_i \in \mathbb{C}^R$ associates a subject and an object with a predicate class and a time period. $\mathbb{C}^O$ and $\mathbb{C}^R$ means the object and predicate classes.

Metric In practice, the output of the PVSG task is to predict a set of triplets to describe the input video. Take a triplet as an example, which contains a relation r_i from t_1 to t_2, associates the subject with its class category o_s and mask tube $\mathbf{m}_s^{(t_1, t_2)}$, and an object with o_s and $\mathbf{m}_o^{(t_1, t_2)}$. $\mathbf{m}^{(t_1, t_2)}$ denotes the mask tube $\mathbf{m}$ span across the period of t_1 to t_2.

To evaluate the PVSG task, we follow the classic SGG and VidSGG paper and use the metrics of the R@K and mR@K, which calculates the triplet recall and mean recall given the top K triplets from the PVSG model. A successful recall of a ground-truth triplet $(\hat{o}_s, \hat{\mathbf{m}}_s^{(\hat{t}_1, \hat{t}_2)}, \hat{o}_s, \hat{\mathbf{m}}_o^{(\hat{t}_1, \hat{t}_2)}, \hat{r}_i^{(\hat{t}_1, \hat{t}_2)})$ should meet the following criteria: 1) the correct category labels of the subject, object, and predicate: 2) the volume IOU between the predicted mask tubes $(\mathbf{m}_s^{(t_1, t_2)}, \mathbf{m}_o^{(t_1, t_2)})$ and the ground-truth tubes $(\mathbf{m}_s^{(\hat{t}_1, \hat{t}_2)}, \mathbf{m}_o^{(\hat{t}_1, \hat{t}_2)})$ should be individually over 0.5. When the previous two criteria are met, a soft recall score of the time IOU between $(\hat{t}_1, \hat{t}_2)$ and (t_1, t_2) is recorded.

Please notice the nuance of the PVSG metrics compared with VidSGG metrics for VidOR [34]. For a case where a child stop-and-go several times in a video, different from VidOR which considers several "child-1 walking on ground" triplets, our PVSG metrics only consider the triplet once, but with a scattered time span. This small change avoids some relations dominating the metrics by repeating.

4. The PVSG Dataset

In this section, we first summarize the existing VidSGG datasets and highlight their problems. Then, we introduce the overview and statistics of our PVSG dataset, and its annotation pipeline.

4.1. Connecting Existing Datasets to PVSG

To select candidate video clips for the PVSG dataset, a go-to option is to borrow the videos from other VidSGG datasets. Table 1 lists three classic VidSGG datasets chronologically. While the limited size of their first VidSGG dataset, ImageNet-VidVRD [35], Shang *et al.* collects 10K videos from the user-uploaded dataset YFCC100M [42] and generate a large-scale VIDOR dataset [34], with dense object and relation annotation. Ji *et al.* also introduces a large-scale dataset Action

Genome (AG) based on a diverse, crowd-sourcing Charades dataset [36]. While Charades provides a novel solution to gather large-scale, less-biased video datasets by asking people to act based on the generated script, the curated scripts usually produce random action series, such as a man rushing out of the room and running back for no reason. Also, the performance traces turn out to be heavy in the dataset. These shortcomings limit the potential of the community to explore contextual logic and reasoning in videos.

Alternative video datasets that lean toward logic reasoning and video scene understanding are instruction datasets or movie datasets. However, these datasets are either full of close-up shots (e.g., Something-Something [11], Howto100M [29]) or cut shots (e.g., MOMA [27], HC-STVG [40]). In fact, humans rely on unpolished videos to form an essential understanding of the world. In this sense, we find that the unedited, natural, and diverse VidOR [34] videos are a good candidate for learning the visual essence as well as keeping the potential of contextual logic exploration. While the videos presented above showcase a third-person perspective, egocentric videos have gained popularity due to their practicality in autonomous driving [54], robotic decision-making [57], and in the metaverse [30]. In particular, a subset of the Ego4D dataset [12] is suitable for exploring logical relationships and modeling, as it supports short and long-term action anticipation tasks. Additionally, the Epic-Kitchens [6] dataset is focused on the kitchen scenario and offers rich action data. Its subset, the VISOR dataset, includes video object segmentation (VOS) annotation, which partially matches the PVSG scope, though its relations are not yet annotated.

Another dataset category that is closely related to the PVSG problem is the video panoptic segmentation (VPS) datasets. Popular VPS datasets include Cityscapes-VPS [17] and KITTI-STEP [45]. However, the relations in the self-driving scenarios are limited, which is not suitable for the PVSG task. Although the recent VIP-Seg [28] provides a more diverse VPS dataset, each video only lasts around 5 seconds, which also lacks temporal relations.

With all the rationale above, we eventually decide to combine three video sources to the PVSG dataset, which are VidOR, Ego4D-STA, and Epic-Kitchens-100 (including some videos from VISOR).

4.2. Dataset Statistics

Figure 2 displays the statistics of the PVSG dataset, which consists of 400 videos, including 289 third-person videos from VidOR and 111 egocentric videos from Epic-Kitchens and Ego4D. Among the videos, 62 videos feature birthday celebrations, while 35 videos center around ceremonies, providing rich content for contextual logic and reasoning. Furthermore, the dataset includes numerous videos related to sports and pets, featuring complex and diverse ac-
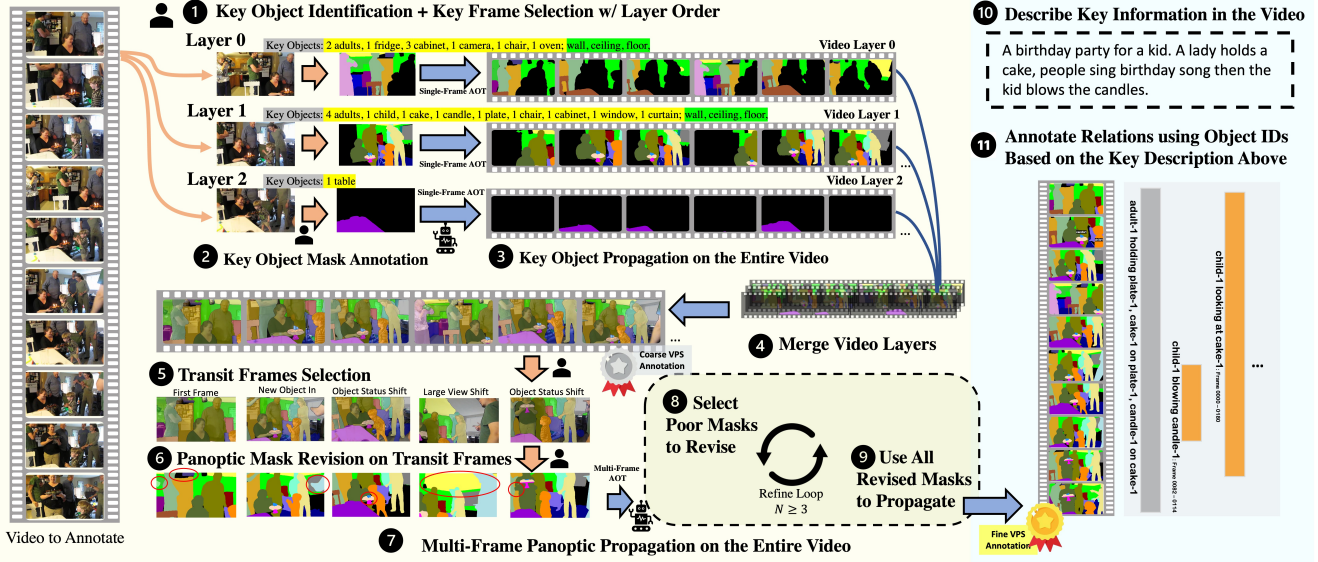
Figure 3. **PVSG Dataset Annotation Pipeline.** The construction of PVSG dataset can be divided into VPS annotation and relation annotation. For VPS annotation, we select a few key frames and use an off-the-shelf video object segmentation (VOS) model AOT [53] to propagate the annotated objects to the whole video, and then perform frame-level mask fusion using the predefined layer order to obtain a coarse VPS annotation for further revision. The relations are annotated based on the description of the key information in the video.

tions and interactions between objects. Figure 2-(c) shows the object count (including stuff) in the PVSG dataset.

4.3. Dataset Construction Pipeline

Creating the PVSG dataset is never a trivial task considering that both video panoptic segmentation and relation annotations are required. This section describes how the PVSG dataset is collected and annotated.

Step 1: Video Clip Selection To get rid of the drawbacks of the current datasets (i.e., the unnatural videos in AG [15] without logical script, and the static and short videos from the VPS datasets), we carefully select around 300 long, daily, unedited videos with a logical storyline. In addition, to encourage the VidSGG models to be practical on egocentric videos, we also select around 100 videos from Epic-Kitchens and Ego4D with the same criteria. Videos with too many small and trivial objects are also discarded for VPS annotation purposes. We hope the selected videos could greatly encourage the exploration of video recognition, understanding, and reasoning.

Step 2: VPS Annotation Notice that the PVSG videos have more than 300 frames on average and 150K in total, it is impossible to annotate panoptic segmentation for each frame. After iterations and improvements, we finalize a human-machine collaborative VPS annotation pipeline, depicted in Figure 3. In a nutshell, we largely rely on an off-the-shelf VOS model called AOT [53] for the human-machine interactive annotation process.

Coarse VPS Annotation: With a few well-annotated ob-

ject masks in the first frame, the AOT [53] is able to propagate the masks to later frames. With this strong automatic tool, we design a pipeline to obtain coarse VPS annotation. For the example video in Figure 3 (actions 1-3), we first identify several key objects to annotate, and also identify key frames where the selected objects have a clear and whole appearance. To identify key objects, our annotators need to select all objects and background to address "panoptic", except those messy and unrelated ones. After annotating these key objects on their corresponding frames, we use AOT based on the frames to propagate the mask, both forward and backward. Thus, each frame will yield a whole mask video. To merge those mask videos into one, the layer order should be considered beforehand, i.e., the objects from which layer should be put in front. In fact, the decision of the layer order is made with key frame selection.

Fine VPS Annotation: Based on the coarse VPS annotation, we conduct several rounds (more than 5) of the human-machine interactive revision process to obtain the final annotation. We rely on the multi-frame panoptic segmentation propagation mode of the AOT algorithm [53], which interpolates the entire video masks based on several frames with the entire panoptic segmentation. The quality of interpolation increases with more intermediate frames. To accelerate the revision process, we revise the transit frames first, as shown in action 5 in Figure 3. Typical examples of poor masks include incorrect tracking masks and boundaries that deviate significantly from the object.

Step 3: Relation Annotation We annotate temporal re-

(a) Stage-1: For Feature Tube and Mask Tube Output   **(b) Stage 2: Relation Prediction**
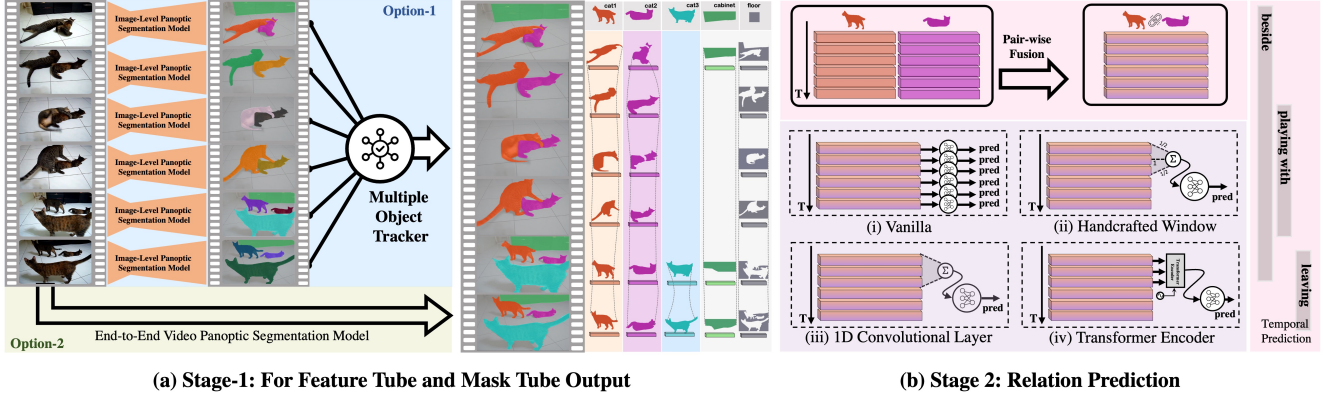
Figure 4. **The two-stage framework to solve the PVSG task.** The goal of the first stage is to obtain the video panoptic segmentation mask for each object, as well as its corresponding video-length feature tube. Two options are provided to achieve the goal. The second stage predicts pairwise relations based on all the feature tubes from the first stage. Four options are provided for a comprehensive comparison.

lations based on the VPS annotation, with object ID prepared. To guarantee the significance of the relation, we ask annotators to describe the video with several sentences and annotate relations accordingly. The relations they use are strictly within our dictionary, but we also enlarge the dictionary when necessary. Similar to the PSG dataset [50], we ask the annotators to use the most unambiguous predicate as possible, i.e., "sitting on" rather than "on".

5. Methodology

In this section, we introduce the two-stage pipeline to address the PVSG problem. We provide two options for the first stage and four options for the second stage.

5.1. Stage One: Video Panoptic Segmentation

Given a video clip input $\mathbf{V} \in \mathbb{R}^{T \times H \times W \times 3}$, the goal of VPS is to segment and track each pixel in a non-overlap manner. Specifically, the model predicts a set of video clips $\{y_i\}_{i=1}^{N} = \{(\mathbf{m}_i, p_i(c))\}_{i=1}^{N}$, where $\mathbf{m}_i \in \{0, 1\}^{T \times H \times W}$ denotes the tracked video mask, and $p_i(c)$ denotes the probability of assigning class c to a clip $\mathbf{m}_i$. N is the number of entities, which includes thing classes and stuff classes.

We present two strong baselines for the first stage of VPS processing. In particular, we adopt the state-of-the-art image segmentation baseline [3] with an extra tracker and the improved video panoptic segmentation method [25]. For the former, it processes the video frames individually. For the latter, it processes the video frames across the temporal dimension, with a nearby frame as the reference frame.

IPS+T: Image Panoptic Segmentation With Tracker We adopt strong Mask2Former [3] as our baseline method since it is a mask-based transformer architecture. It contains a transformer encoder-decoder architecture with a set of object queries, where the object queries interact with encoder features via masked cross-attention. Given an image

$\mathbf{I}$, during the inference, the Mask2Former directly outputs a set of object queries $\{q_i\}, i = 1, \ldots, N$, where each object query q_i represent one entity. Then, two different Multiple Layer Perceptrons (MLPs) project the queries into two embeddings for mask classification and mask prediction, respectively. During training, each object query is matched to ground truth masks via masked-based bipartite matching.

We first fine-tune the Mask2Former on our dataset. Then, we test the model with an extra tracker [44]. In particular, we first obtain panoptic segmentation results of each frame. Then we link each frame via using UniTrack [44] for tracking to obtain the final N tracked video cubes for each clip. Therefore, a query tube is obtained. For the object i at the t-th frame, the query is noted as q_i^t. We use $\mathbb{Q}_i^{(t_1, t_2)}$ to denote the set of queries $\{q_i^t\}_{t=t_1}^{t_2}$, and $\mathbb{Q}_i$ denotes the query tube in the entire video.

VPS: Video Panoptic Segmentation Baseline For video baselines, we modify the previous state-of-the-art method Video K-Net [25] into Mask2Former framework. We first replace the backbone and neck in Video K-Net [25] with Mask2Former feature extractor. Then we use the temporal contrastive loss to directly on the output queries from the last layer of the decoder. In particular, given two frames, we first obtained the object queries from both frames, and then we sent them into an embedding layer (a shared MLP) to obtain association embeddings. We adopt the same tracking loss used in [25] to supervise the association embeddings. The embeddings are close if they are the same object, otherwise, they are pulled away.

During the training, the two nearby frames are sent to the model to learn the association embedding. During the inference, the learned association embeddings are used to perform instance-wised tracking cues to match each thing masks frame by frame in an online manner. Compared with the image baseline, our video baseline considers the tempo-

Table 2. **Comparison between all two-stage PVSG baselines.** We provide two options for the first stage and four options for the second stage, as described in Section 3. The results show that using the basic image-based method in the first stage with the transformer encoder in the second stage can achieve the optimal recall.

Method		PVSG Metrics		
Stage-1	Stage-2	R/mR@20	R/mR@50	R/mR@100
IPS+T [3, 44]	Vanilla	2.35 / 1.22	2.71 / 1.31	2.94 / 1.45
	Handcrafted Window	2.56 / 1.24	2.78 / 1.35	3.05 / 1.54
	1D Convolution	2.79 / 1.24	2.80 / 1.47	3.10 / 1.59
	Transformer Encoder	**4.02 / 1.75**	**4.41 / 1.86**	**4.88 / 2.03**
VPS [3, 25]	Vanilla	0.52 / 0.24	0.60 / 0.24	0.63 / 0.24
	Handcrafted Window	0.54 / 0.27	0.61 / 0.29	0.62 / 0.29
	1D Convolution	0.60 / 0.27	0.73 / 0.28	0.76 / 0.29
	Transformer Encoder	**0.75 / 0.36**	**0.91 / 0.39**	**0.94 / 0.40**

ral learned embedding. After this step, we obtain N tracked video cubes for each clip. For both baselines, we also dump the corresponding object queries for further processing.

5.2. Stage Two: Relation Classification

The object query (feature) tubes $\{Q_i\}_{i=1}^N$ serve as a link between the first and second stages. Object tubes are paired with each other in their intersections in the second stage, as in Figure 4. Specifically, as in Figure 4 (b), we first concatenate the query pairs. Next, we mainly introduce four operations to process the relations between feature pairs.

Vanilla: Fully-Connected Layer Begin with the most basic version, the pairwise feature fusion is followed by a straightforward fully-connected layer on the fused features. In this scenario, some objects may have several interactions occurring simultaneously, we define the issue as a multi-label classification job with binary cross-entropy loss.

Handcrafted Filter To further consider the temporal information, we design a simple kernel to gather the information from the context in nearby frames. By default, the handcrafted filter is a simple vector of $[1/4, 1/2, 1, 1/2, 1/4]$ with a window size of 5. Note that the filter is also required during inference.

1D-Convolutional Layer To improve the handcrafted filter, we also utilize a learnable 1D-Convolutional layer to capture temporal information. The kernel sizes are set to 5 in 3 layers.

Transformer Encoder A transformer encoder [43] is also suitable in this scenario. We utilize a 3-layer transformer block with positional embeddings in the entire fused query feature to capture temporal information via cross-attention between frames.

6. Experiments

In this section, we show the experimental results for the PVSG dataset. We split the dataset with 360 videos for

training and 40 videos for testing. For both IPS+T and VPS, we adopt Mask2Former upon the ResNet-50 [13] backbone with 12 training epochs, which takes 12 hours and 48 hours on 8 V-100 GPUs, respectively. The training time of the second stage is shorter than an hour on single V-100 GPU.

The experimental results to compare two stage-one options and four stage-two options are shown in Table 2. We first take a look at the second stage. The transformer encoder obtains the optimal results regardless of the first-stage options, showing the effectiveness of temporal information fusion. Besides, the 1D convolutional layer achieves better results than the handcrafted window, showing that modeling with learning parameters in the second stage is worth exploring. Considering the harsh recall criteria described in Section 3, even the most basic vanilla method can achieve a few recall scores, showing that the PVSG task is solvable with a decent first-stage model. We hope that the second stage alone could advance research efforts on visual temporal predictions.

We then discuss the influence of the first stage. According to Table 2, the end-to-end VPS model seems to underperform the IPS+T baseline. Although the VPS models are shown effective on the existing VPS datasets such as Cityscape-VPS and Kitty-STEP, videos in the PVSG dataset are longer and more dynamic (frequent and large camera view shift), which seems to bring new challenges for the VPS community. According to Figure 5, the end-to-end VPS model fails to achieve a higher tracking performance, which seems severely affect its performance on the PVSG task.

7. Conclusion, Challenges, and Outlook

In this paper, we introduce a new PVSG task, a new PVSG dataset with several baselines to address the new task, in hope of encouraging comprehensive video understanding and trigger more interesting downstream tasks such as visual reasoning. Here we discuss the challenges
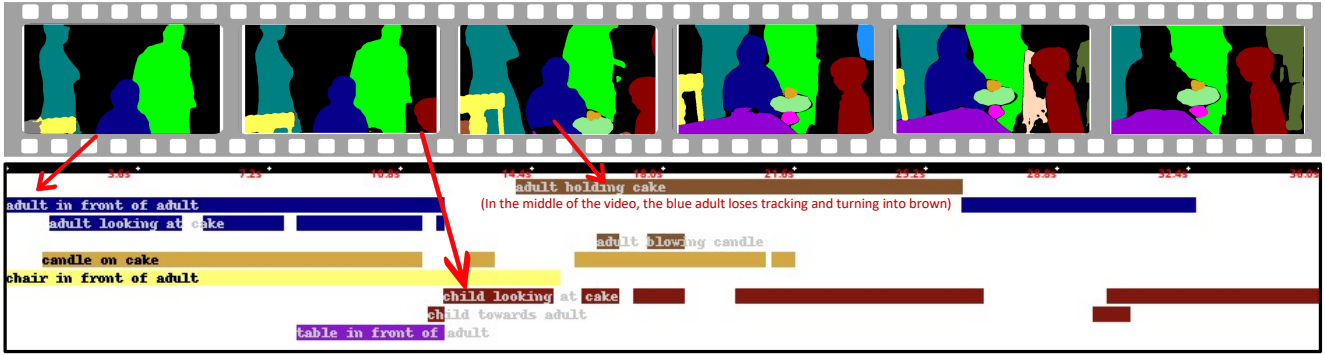
(a) The visualization result with the IPS+T method in the first stage and Transformer Encoder in the second stage.

(b) The visualization result with the VPS method in the first stage and Transformer Encoder in the second stage.

Figure 5. **The visualization of the top triplets generated by PVSG models.** The result shows that the IPS+T method is able to predict a better-quality video panoptic mask. The VPS baseline is shown unable to perform well on tracking (e.g., the tracking of the child switched in the later frames), which leads to its low performance in the PVSG task.

and future work.

Challenges Real-world data often exhibit long-tailed heteroscedastic distributions across objects and relations, as shown in Figure 2. The PVSG models are expected to predict informative and diverse relations, rather than being obsessed with statistically common relations. Yet another challenge the PVSG models faces is the aleatoric uncertainty in verbal relation descriptions. For example, "playing with" can be overlapping with "chasing" when it describes two kids chasing each other. Such nuances from canonical languages introduce intrinsic label noises in prevailing video event datasets, including PVSG. Another important challenge that the PVSG dataset introduces is video panoptic segmentation. With the video with a large view shift, the VPS models are expected to have a better performance on tracking and segmentation.

Outlook on Video Perception and Reasoning We foresee the potential of PVSG in bridging video scene perception and reasoning. While current video question-answering datasets lack pixel-level segmentation masks that refine (sometimes determine) the relations between object pairs, the inclusion of such dense annotations is critical to video reasoning tasks. PVSG is related to social intelligence, with rich event annotations in human behaviors and dynamics. In the same spirit, it is also related to human-object interaction (HOI) that dense labels are capable to capture very subtle visual differences in the scene.

Potential Negative Societal Impacts This work releases a dataset containing human behaviours, posing possible gender and social biases inherently from data. Potential users are encouraged to consider the risks of oversighting ethical issues in imbalanced data, especially in underrepresented minority classes.

[1] https:// ngm mthuk u0w g. o ibee oo .rest/

References

[1] Jin Chen, Xiaofeng Ji, and Xinxiao Wu. Adaptive image-to-video scene graph generation via knowledge reasoning and adversarial learning. 2022. 1, 3

[2] Bowen Cheng, Maxwell D Collins, Yukun Zhu, Ting Liu, Thomas S Huang, Hartwig Adam, and Liang-Chieh Chen. Panoptic-deeplab: A simple, strong, and fast baseline for bottom-up panoptic segmentation. In *CVPR*, 2020. 3

[3] Bowen Cheng, Ishan Misra, Alexander G. Schwing, Alexander Kirillov, and Rohit Girdhar. Masked-attention mask transformer for universal image segmentation. 2022. 6, 7

[4] Yuren Cong, Michael Ying Yang, and Bodo Rosenhahn. Reltr: Relation transformer for scene graph generation. *arXiv preprint arXiv:2201.11460*, 2022. 2

[5] Marius Cordts, Mohamed Omran, Sebastian Ramos, Timo Rehfeld, Markus Enzweiler, Rodrigo Benenson, Uwe Franke, Stefan Roth, and Bernt Schiele. The cityscapes dataset for semantic urban scene understanding. In *CVPR*, 2016. 3

[6] Dima Damen, Hazel Doughty, Giovanni Maria Farinella, Sanja Fidler, Antonino Furnari, Evangelos Kazakos, Davide Moltisanti, Jonathan Munro, Toby Perrett, Will Price, et al. Scaling egocentric vision: The epic-kitchens dataset. In *ECCV*, 2018. 4

[7] Dima Damen, Hazel Doughty, Giovanni Maria Farinella, Antonino Furnari, Evangelos Kazakos, Jian Ma, Davide Moltisanti, Jonathan Munro, Toby Perrett, Will Price, et al. Epic-kitchens-100. *International Journal of Computer Vision*, 130:33–55, 2022. 2

[8] Ahmad Darkhalil, Dandan Shan, Bin Zhu, Jian Ma, Amlan Kar, Richard Ely Locke Higgins, Sanja Fidler, David Fouhey, and Dima Damen. Epic-kitchens visor benchmark: Video segmentations and object relations. In *NeurIPS*, 2022. 2

[9] Linsen Dong, Guanyu Gao, Xinyi Zhang, Liangyu Chen, and Yonggang Wen. Baconian: A unified open-source framework for model-based reinforcement learning, 2021. 3

[10] Amy Fire and Song-Chun Zhu. Learning perceptual causality from video. *ACM Transactions on Intelligent Systems and Technology (TIST)*, 7(2):1–22, 2015. 2

[11] Raghav Goyal, Samira Ebrahimi Kahou, Vincent Michalski, Joanna Materzynska, Susanne Westphal, Heuna Kim, Valentin Haenel, Ingo Fruend, Peter Yianilos, Moritz Mueller-Freitag, et al. The" something something" video database for learning and evaluating visual common sense. In *ICCV*, 2017. 4

[12] Kristen Grauman, Andrew Westbury, Eugene Byrne, Zachary Chavis, Antonino Furnari, Rohit Girdhar, Jackson Hamburger, Hao Jiang, Miao Liu, Xingyu Liu, et al. Ego4d: Around the world in 3,000 hours of egocentric video. In *Proceedings of the IEEE/CVF Conference on Computer Vision and Pattern Recognition*, pages 18995–19012, 2022. 2, 4

[13] Kaiming He, Xiangyu Zhang, Shaoqing Ren, and Jian Sun. Deep residual learning for image recognition. In *Proceedings of the IEEE conference on computer vision and pattern recognition*, pages 770–778, 2016. 7

[14] Samitha Herath, Mehrtash Harandi, and Fatih Porikli. Going deeper into action recognition: A survey. *Image and vision computing*, 60:4–21, 2017. 2

[15] Jingwei Ji, Ranjay Krishna, Li Fei-Fei, and Juan Carlos Niebles. Action genome: Actions as compositions of spatiotemporal scene graphs. In *CVPR*, 2020. 1, 2, 5

[16] Justin Johnson, Ranjay Krishna, Michael Stark, Li-Jia Li, David Shamma, Michael Bernstein, and Li Fei-Fei. Image retrieval using scene graphs. In *CVPR*, 2015. 1

[17] Dahun Kim, Sanghyun Woo, Joon-Young Lee, and In So Kweon. Video panoptic segmentation. In *Proceedings of the IEEE/CVF Conference on Computer Vision and Pattern Recognition*, pages 9859–9868, 2020. 2, 4

[18] Dahun Kim, Sanghyun Woo, Joon-Young Lee, and In So Kweon. Video panoptic segmentation. In *CVPR*, 2020. 3

[19] Dahun Kim, Jun Xie, Huiyu Wang, Siyuan Qiao, Qihang Yu, Hong-Seok Kim, Hartwig Adam, In So Kweon, and Liang-Chieh Chen. Tubeformer-deeplab: Video mask transformer. In *CVPR*, 2022. 3

[20] Alexander Kirillov, Kaiming He, Ross Girshick, Carsten Rother, and Piotr Dollár. Panoptic segmentation. In *Proceedings of the IEEE/CVF Conference on Computer Vision and Pattern Recognition*, pages 9404–9413, 2019. 2

[21] Ranjay Krishna, Yuke Zhu, Oliver Groth, Justin Johnson, Kenji Hata, Joshua Kravitz, Stephanie Chen, Yannis Kalantidis, Li-Jia Li, David A Shamma, Michael Bernstein, and Li Fei-Fei. Visual genome: Connecting language and vision using crowdsourced dense image annotations. *IJCV*, 2017. 3

[22] Lin Li, Long Chen, Yifeng Huang, Zhimeng Zhang, Songyang Zhang, and Jun Xiao. The devil is in the labels: Noisy label correction for robust scene graph generation. In *CVPR*, 2022. 3

[23] Rongjie Li, Songyang Zhang, and Xuming He. Sgtr: End-to-end scene graph generation with transformer. In *Proceedings of the IEEE/CVF Conference on Computer Vision and Pattern Recognition*, pages 19486–19496, 2022. 2

[24] Xinghang Li, Di Guo, Huaping Liu, and Fuchun Sun. Embodied semantic scene graph generation. In *Conference on Robot Learning*, pages 1585–1594. PMLR, 2022. 1, 3

[25] Xiangtai Li, Wenwei Zhang, Jiangmiao Pang, Kai Chen, Guangliang Cheng, Yunhai Tong, and Chen Change Loy. Video k-net: A simple, strong, and unified baseline for video segmentation. In *CVPR*, 2022. 3, 6, 7

[26] Chenchen Liu, Yang Jin, Kehan Xu, Guoqiang Gong, and Yadong Mu. Beyond short-term snippet: Video relation detection with spatio-temporal global context. In *Proceedings of the IEEE/CVF conference on computer vision and pattern recognition*, pages 10840–10849, 2020. 3

[27] Zelun Luo, Wanze Xie, Siddharth Kapoor, Yiyun Liang, Michael Cooper, Juan Carlos Niebles, Ehsan Adeli, and Fei-Fei Li. Moma: Multi-object multi-actor activity parsing. *NeurIPS*, 2021. 4

[28] Jiaxu Miao, Xiaohan Wang, Yu Wu, Wei Li, Xu Zhang, Yunchao Wei, and Yi Yang. Large-scale video panoptic segmentation in the wild: A benchmark. In *CVPR*, 2022. 2, 3, 4

[29] Antoine Miech, Dimitri Zhukov, Jean-Baptiste Alayrac, Makarand Tapaswi, Ivan Laptev, and Josef Sivic.

HowTo100M: Learning a Text-Video Embedding by Watching Hundred Million Narrated Video Clips. In *ICCV*, 2019. 4

[30] Beng Chin Ooi, Kian-Lee Tan, Anthony Tung, Gang Chen, Mike Zheng Shou, Xiaokui Xiao, and Meihui Zhang. Sense the physical, walkthrough the virtual, manage the metaverse: A data-centric perspective. *arXiv preprint arXiv:2206.10326*, 2022. 4

[31] Xufeng Qian, Yueting Zhuang, Yimeng Li, Shaoning Xiao, Shiliang Pu, and Jun Xiao. Video relation detection with spatio-temporal graph. In *Proceedings of the 27th ACM International Conference on Multimedia*, pages 84–93, 2019. 3

[32] Siyuan Qiao, Yukun Zhu, H. Adam, A. Yuille, and Liang-Chieh Chen. Vip-deeplab: Learning visual perception with depth-aware video panoptic segmentation. *CVPR*, 2021. 3

[33] Olga Russakovsky, Jia Deng, Hao Su, Jonathan Krause, Sanjeev Satheesh, Sean Ma, Zhiheng Huang, Andrej Karpathy, Aditya Khosla, Michael Bernstein, et al. Imagenet large scale visual recognition challenge. *IJCV*, 2015. 2

[34] Xindi Shang, Donglin Di, Junbin Xiao, Yu Cao, Xun Yang, and Tat-Seng Chua. Annotating objects and relations in user-generated videos. In *ICMR*, 2019. 2, 4

[35] Xindi Shang, Tongwei Ren, Jingfan Guo, Hanwang Zhang, and Tat-Seng Chua. Video visual relation detection. In *ACM MM*, 2017. 2, 3, 4

[36] Gunnar A Sigurdsson, Gül Varol, Xiaolong Wang, Ali Farhadi, Ivan Laptev, and Abhinav Gupta. Hollywood in homes: Crowdsourcing data collection for activity understanding. In *ECCV*, 2016. 2, 4

[37] Zixuan Su, Xindi Shang, Jingjing Chen, Yu-Gang Jiang, Zhiyong Qiu, and Tat-Seng Chua. Video relation detection via multiple hypothesis association. In *Proceedings of the 28th ACM International Conference on Multimedia*, pages 3127–3135, 2020. 3

[38] Mohammed Suhail, Abhay Mittal, Behjat Siddiquie, Chris Broaddus, Jayan Eledath, Gerard Medioni, and Leonid Sigal. Energy-based learning for scene graph generation. In *CVPR*, 2021. 2

[39] Kaihua Tang, Hanwang Zhang, Baoyuan Wu, Wenhan Luo, and Wei Liu. Learning to compose dynamic tree structures for visual contexts. In *CVPR*, 2019. 2

[40] Zongheng Tang, Yue Liao, Si Liu, Guanbin Li, Xiaojie Jin, Hongxu Jiang, Qian Yu, and Dong Xu. Human-centric spatio-temporal video grounding with visual transformers. *IEEE TCSVT*, 2021. 4

[41] Yao Teng, Limin Wang, Zhifeng Li, and Gangshan Wu. Target adaptive context aggregation for video scene graph generation. In *Proceedings of the IEEE/CVF International Conference on Computer Vision*, pages 13688–13697, 2021. 1, 3

[42] Bart Thomee, David A Shamma, Gerald Friedland, Benjamin Elizalde, Karl Ni, Douglas Poland, Damian Borth, and Li-Jia Li. Yfcc100m: The new data in multimedia research. *Communications of the ACM*, 2016. 2, 4

[43] Ashish Vaswani, Noam Shazeer, Niki Parmar, Jakob Uszkoreit, Llion Jones, Aidan N Gomez, Łukasz Kaiser, and Illia Polosukhin. Attention is all you need. *NeurIPS*, 2017. 7

[44] Zhongdao Wang, Hengshuang Zhao, Ya-Li Li, Shengjin Wang, Philip HS Torr, and Luca Bertinetto. Do different tracking tasks require different appearance models? *NeurIPS*, 2021. 6, 7

[45] Mark Weber, Jun Xie, Maxwell Collins, Yukun Zhu, Paul Voigtlaender, Hartwig Adam, Bradley Green, Andreas Geiger, Bastian Leibe, Daniel Cremers, et al. Step: Segmenting and tracking every pixel. *arXiv preprint arXiv:2102.11859*, 2021. 2, 4

[46] M. Weber, J. Xie, M. Collins, Yukun Zhu, P. Voigtlaender, H. Adam, B. Green, A. Geiger, B. Leibe, D. Cremers, Aljosa Osep, L. Leal-Taixé, and Liang-Chieh Chen. Step: Segmenting and tracking every pixel. *NIPS*, 2021. 3

[47] Sanghyun Woo, Dahun Kim, Joon-Young Lee, and In So Kweon. Learning to associate every segment for video panoptic segmentation. In *CVPR*, 2021. 3

[48] Danfei Xu, Yuke Zhu, Christopher B Choy, and Li Fei-Fei. Scene graph generation by iterative message passing. In *CVPR*, 2017. 1, 2

[49] Li Xu, Haoxuan Qu, Jason Kuen, Jiuxiang Gu, and Jun Liu. Meta spatio-temporal debiasing for video scene graph generation. In *European Conference on Computer Vision*, pages 374–390. Springer, 2022. 1, 3

[50] Jingkang Yang, Yi Zhe Ang, Zujin Guo, Kaiyang Zhou, Wayne Zhang, and Ziwei Liu. Panoptic scene graph generation. In *European Conference on Computer Vision*, pages 178–196. Springer, 2022. 1, 2, 3, 6

[51] Jianwei Yang, Jiasen Lu, Stefan Lee, Dhruv Batra, and Devi Parikh. Graph r-cnn for scene graph generation. In *ECCV*, 2018. 1

[52] Linjie Yang, Yuchen Fan, and Ning Xu. Video instance segmentation. In *ICCV*, 2019. 3

[53] Zongxin Yang, Yunchao Wei, and Yi Yang. Associating objects with transformers for video object segmentation. In *NeurIPS*, 2021. 5

[54] Yu Yao, Mingze Xu, Chiho Choi, David J Crandall, Ella M Atkins, and Behzad Dariush. Egocentric vision-based future vehicle localization for intelligent driving assistance systems. In *2019 International Conference on Robotics and Automation (ICRA)*, pages 9711–9717. IEEE, 2019. 4

[55] Haobo Yuan, Xiangtai Li, Yibo Yang, Guangliang Cheng, Jing Zhang, Yunhai Tong, Lefei Zhang, and Dacheng Tao. Polyphonicformer: Unified query learning for depth-aware video panoptic segmentation. In *ECCV*, 2022. 3

[56] Rowan Zellers, Mark Yatskar, Sam Thomson, and Yejin Choi. Neural motifs: Scene graph parsing with global context. In *CVPR*, 2018. 2

[57] Jingzhe Zhang, Lishuo Zhuang, Yang Wang, Yameng Zhou, Yan Meng, and Gang Hua. Video demo: An egocentric vision based assistive co-robot. In *Proceedings of the IEEE Conference on Computer Vision and Pattern Recognition Workshops*, pages 48–49, 2013. 4

[58] Yiwu Zhong, Jing Shi, Jianwei Yang, Chenliang Xu, and Yin Li. Learning to generate scene graph from natural language supervision. In *ICCV*, 2021. 2

[59] Bolei Zhou, Alex Andonian, Aude Oliva, and Antonio Torralba. Temporal relational reasoning in videos. In *Proceed-*

ings of the European conference on computer vision (ECCV), pages 803–818, 2018. 2